Thermal shock fragmentation of Mg silicates within scoriaceous micrometeorites reveal hydrated asteroidal sources

Matthew J. Genge[1,2]*, Martin Suttle[1,2], and Matthias Van Ginneken[3]

[1]Impact and Astromaterials Research Centre (IARC), Department of Earth Science and Engineering, Imperial College London, Exhibition Road, London SW7 2AZ, UK
[2]Earth Sciences Department, The Natural History Museum, Cromwell Road, London SW7 2BW, UK
[3]Earth System Science, Vrije Universiteit Brussel, Pleinlaan, 2 B-1050 Brussel, Belgium

ABSTRACT

Scoriaceous micrometeorites are highly vesicular extraterrestrial dust particles that have experienced partial melting during atmospheric entry. We report the occurrence of clusters of anhedral relict forsterite crystals within these particles that testify to in situ fragmentation. The absence of similar clusters within unmelted micrometeorites suggests that fragmentation occurs during atmospheric entry rather than by parent body shock reprocessing. Clusters of broken forsterite crystals are shown to form as a result of fracturing owing to thermal stress developed during entry heating and require thermal gradients of >200 K μm^{-1} in order for differential thermal expansion to exceed the critical shear strength of olivine. Thermal gradients of this magnitude significantly exceed those resulting from thermal conduction and require the endothermic decomposition of phyllosilicates. Fragmented relict forsterite within scoriaceous micrometeorites, therefore, indicate that the precursor grains were similar to CI and CM2 chondrites and retained phyllosilicate prior to atmospheric entry and thus were not dehydrated on the parent asteroid by shock or thermal metamorphism. Explosive fragmentation of hydrous asteroids during collisions, therefore, does not significantly bias the interplanetary dust population.

INTRODUCTION

Micrometeorites (MMs) are extraterrestrial dust particles <2 mm in size that are recovered from Earth's surface (Genge et al., 2008), they have been collected from Antarctic blue ice and snow, Antarctic traps and aeolian deposits (Maurette et al., 1991; Taylor et al., 2000; Duprat et al., 2007; Rochette et al., 2008), and within deep-sea sediments (Brownlee and Bates, 1983). The majority of MMs are thought to be derived from primitive asteroids similar to the parent bodies of chondrites (Kurat et al., 1994; Genge et al., 1997, 2008; Genge, 2008; Cordier et al., 2011), although some particles are also from comets (Noguchi et al., 2015).

A large proportion of MMs experience significant heating during atmospheric entry to form partially melted scoriaceous particles and extensively melted cosmic spherules (Kurat et al., 1994; Genge et al., 2008; Taylor et al., 2011). Heating during atmospheric entry obscures the pre-atmospheric features of MMs. In most unmelted fine-grained particles phyllosilicates are dehydrated and either form dehydroxylates or have recrystallized to cryptocrystalline olivine (Genge et al., 1997; Noguchi et al., 2002; Nozaki et al., 2006; Genge et al., 2008). Dehydration is likely to occur due to atmospheric entry; however, it is also affects dark inclusions (Kojima et al., 1993), and CI, CM, and CK4 chondrites (Nakamura, 2005; Greenwood et al., 2010; Tonui, 2014) and thus occurs on asteroids. Scoriaceous MMs (ScMMs) are thought to have similar pre-atmospheric precursors to unmelted fine-grained MMs but have experienced partial melting of their fine-grained portions, with Mg-rich relict forsterite and enstatite surviving without melting (Genge et al., 1997; Taylor et al., 2011).

Here we report clusters of anhedral relict forsterite and enstatite crystals within ScMMs formed by in situ fragmentation during entry heating. We show that fracturing by thermal stress results from high thermal gradients enabled by phyllosilicates and indicates that particles were still hydrated when they entered the atmosphere.

OBSERVATIONS OF SCORIACEOUS MICROMETEORITES

We examined 91 ScMMs from Cap Prudhomme (Maurette et al., 1991), Larkman Nunatak (Suttle et al., 2015), and Allan Hills Moraine in Antarctica, among a total of 1600 MMs ranging in maximum dimensions from 55 to 450 µm (Fig. 1). Scoriaceous MMs are dominated by micron-sized equant iron-rich olivine crystals within a glassy mesostasis. Vesicles are abundant in these particles comprising 20–70 vol% and consisting of spherical voids to rounded irregular cavities. Some ScMMs have areas of porous mesostasis lacking iron-rich olivine (Fig. 1A) that have previously been interpreted as largely unmelted matrix (Genge et al., 1997). Particle shapes range from irregular and rounded to sub-spherical particles that resemble cosmic spherules. Well-developed magnetite rims, up to 4 µm in thickness, are developed on most ScMMs.

Accessory phases within ScMMs include FeNi-sulfide and FeNi-metal (occurring in 34 particles) and rare chromite and eskolaite (2 particles). Forsterite (Fa_{1-7}) and enstatite (Fs_{1-6}) are relatively common within ScMMs (37% of particles) and occur as grains up to 80 µm in size. Enstatite usually has rims of iron-bearing olivine (Fa_{25-40}). Forsterite and enstatite both often occur as spatially associated clusters of anhedral crystals with smaller grains having shard-like triangular cross-sections (76% of particles with relict Mg silicates). Clusters are defined here as groups of three or more crystals of the same mineral with the same composition with separations less than the average dimensions of the crystals. Two crystals are considered a cluster where their shapes are compatible with in situ fragmentation. Clusters of up to 15 separate grains occur, although those with 3–4 are more common. Small fragments (<5 µm) are often present close to the margins of larger crystals. In some cases veins containing mesostasis up to 5 µm wide penetrate enstatite and forsterite crystals (Fig. 1C).

FORMATION OF FORSTERITE AND ENSTATITE CLUSTERS

The occurrence of clusters of forsterite and enstatite crystals within ScMMs suggests in situ fragmentation, while their absence within unmelted MMs suggests fragmentation occurs during atmospheric entry, rather than parent body shock. Although fractured crystals are common within chondritic meteorites, clusters of these crystals are rare. The texture of particle CP94–050–109 (Figs. 1E and 1F) suggests strongly that fragmentation occurs during entry heating since fractures are observed within relict forsterite where it is in contact with an igneous rim that formed during atmospheric entry (Genge, 2006). Fractures in forsterite
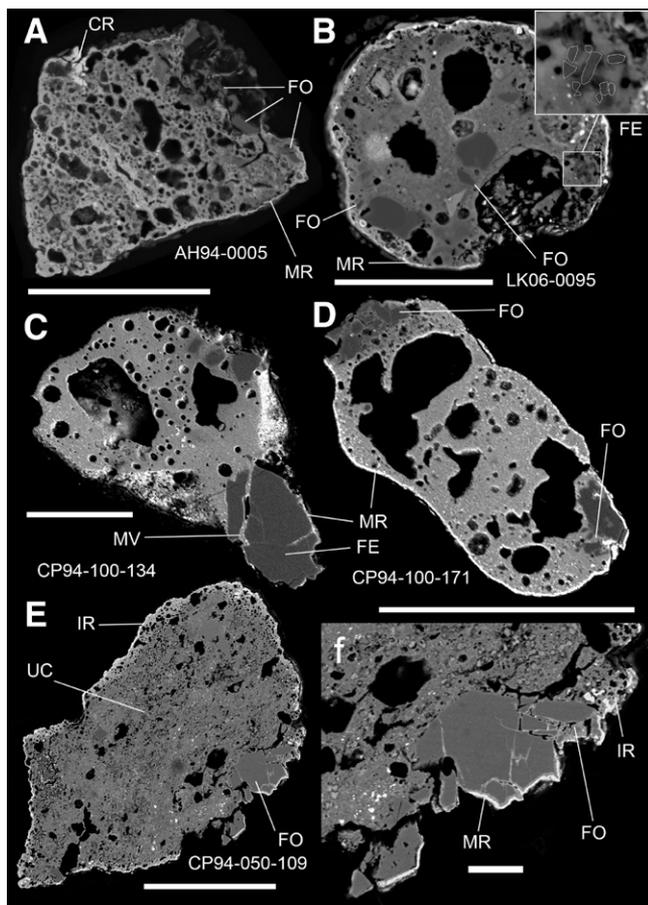
*E-mail: m.genge@imperial.ac.uk

Figure 1. Backscattered electron images of micrometeorites. A: Highly vesicular scoriaceous micrometeorite (ScMM) containing a cluster of forsterite relicts (FO) and eskoliate (Cr$_2$O$_3$ - CR). B: A ScMM with a well-developed external magnetite rim and clusters of forsterite (FO). Small triangular shards of forsterite are present close to larger crystals. This particle is similar to a micro-porphyritic olivine cosmic spherule. An expanded inset shows a cluster of small enstatite crystals. C: A ScMM containing abundant vesicles and a magnetite rim. Two areas of relicts occur, one enstatite (FE) exhibits abundant fractures partially infilled with mesostasis (MV). D: A ScMM containing two clusters of forsterites (FO) consisting of numerous individual crystals. E: An unmelted fine-grained MM with an external igneous rim (IR) surrounding an unmelted core (UC). A forsterite relict (FO) is present that truncates the igneous rim (f shows expanded view) and contains numerous fractures partially infilled with melt and is surrounded by a magnetite rim (MR). Fracturing within the crystal is most abundant in the part closest to the surface of the particle. Scale bars are 50 μm, except in F where it is 5 μm.
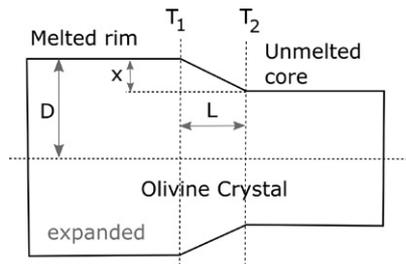

Figure 2. A schematic diagram illustrating the thermal stress model. An olivine crystal is shown that experiences differential thermal expansion across a thermal gradient between the melted (igneous) rim and unmelted core of a micrometeorite.

in this particle are partially filled with melt from the igneous rim similar to relict olivines within some ScMMs (Fig. 1C). Thermal stress resulting from differential thermal expansion of crystals by rapid heating is thus likely to be responsible for the formation of these grains.

Thermal stress between a crystal and its surroundings arises whenever a material expands or contracts owing to temperature change. If confined, thermal stress is dispersed between the expanding material and the surrounding medium, for example, within a melt as in ScMMs, thermal stress is dissipated by expansion (Kingery, 1955). Thermal gradients, however, result in intra-crystal stress due to differential thermal expansion of a single crystal (Yatsu, 1988). Whether thermal stress can cause fragmentation of olivine and enstatite crystals within ScMMs depends on whether these particles have sufficiently large thermal gradients.

A simple model of thermal shock can be constructed by considering expansion of a crystal that is subjected to a thermal gradient oriented orthogonal to its length (Fig. 2). The width of the crystal in the high temperature portion will be larger than in the low temperature region by an amount x that is dependent only on the linear thermal expansion coefficient α, the temperature difference ΔT across the thermal gradient, and the half width of the crystal D, as shown in Equation 1. Expansion along the length of the crystal can be ignored as long as the width of the thermal boundary layer L is small in comparison to the half width of the crystal.

$$x = \alpha D \Delta T. \tag{1}$$

A shear strain is generated within the crystal that has a maximum value at the crystal surface and a magnitude given by x/L. In contrast shear strain is zero at the center of the crystal. Maximum shear stress can be estimated from the strain using the shear modulus G of the crystal. An expression for the width of the thermal boundary layer L is shown in Equation 2.

$$L = \frac{\alpha G \Delta T}{\sigma_{shear}} D. \tag{2}$$

Given an estimate for the critical shear stress, the magnitude of the thermal gradient that causes fragmentation can be estimated. The properties of forsterite are better constrained than those of enstatite. Using G = 80 GPa (Núñez-Valdez et al., 2010), α = 8.7 K^{-1} (Bouhifd et al., 1996), and a critical shear stress of 2.64 GPa (Sammis and Ben-Zion, 2008), the maximum width of the thermal boundary layer that will cause fragmentation for different temperature differences are shown in Figure 3. The thermal gradients required are large with >175 K μm^{-1} required to cause thermal fracturing of olivine crystals 10 μm in width.

The magnitude of thermal gradients that can be supported within micrometeoroids during atmospheric flight by thermal conduction are very small and insufficient to cause thermal fracturing. Steady-state thermal finite-element analysis was performed using the finite element LISA package (http://www.lisa-fet.com) in two dimensions for the mid-plane of a 200 μm sphere with a low thermal conductivity of 0.5 W K^{-1} m^{-2}, corresponding to carbonaceous chondrites (Opeil et al., 2012) and suggests a maximum temperature difference of 49 K over the diameter of the particle where the leading surface is at 1573 K.

The presence of igneous rims on some unmelted MMs (Fig. 1E), however, suggest temperature differences of up to 800 K over a few microns can exist in micrometeoroids during entry heating (Genge, 2006). Igneous rims are thought to develop since the endothermic dehydration of phyllosilicates provides a heat sink, resulting in the inward migration of a melt front into the particle.

To investigate the magnitude of the thermal gradients produced by thermal decomposition of phyllosilicates a one-dimensional finite element analysis of heat flow was performed. Heat flow was modeled from the inner margin of a melted rim, at a solidus temperature of 1573 K, by thermal conduction into the unmelted core of the particle assuming a density of 2400 kg m^{-3}, thermal conductivity of 0.5 K^{-1} and a heat capacity of 550 J kg^{-1} K^{-1} similar to predictions for carbonaceous chondrites (Opeil et al., 2012). Fine-grained MMs contain both serpentine and saponite (e.g., Noguchi et al., 2002; Genge et al., 2008). The kinetics of serpentine dehydration were modeled, in the absence of saponite data, assumed applicable to phyllosilicates in general. The near ubiquitous occurrence
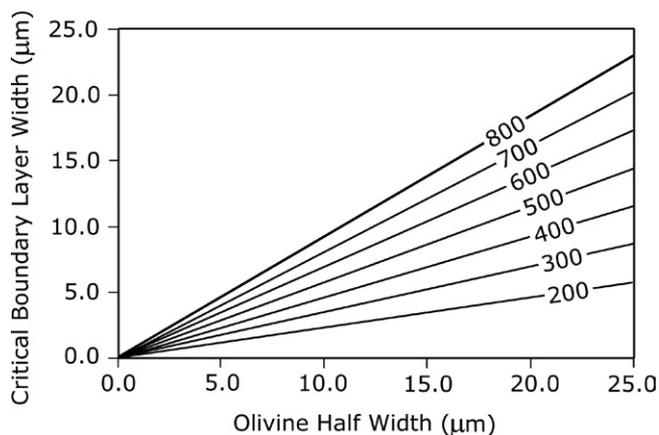
Figure 3. The distance over which a thermal gradient must be applied to cause fracturing of olivine crystals of different widths. Each curve represents the temperature difference in Kelvins of the thermal gradient. Small difference will result from the 0.4% variation in thermal expansivity with crystallographic orientation (Bouhifd et al., 1996).

Figure 4. The results of one-dimensional transient, heat transfer simulations incorporating the kinetics of serpentine decomposition. **A:** Thermal gradient after 0.01 s for matrix with different phyllosilicate contents (in percent). **B:** The evolution of thermal gradient with time for a phyllosilicate-free matrix in comparison to phyllosilicate-dominated at 0.01 s. Percentages of phyllosilicate are shown. Units of axes are the same for A and B.

of igneous rims on heated fine-grained MMs supports similar behavior of saponite and serpentine. Experimentally determined reaction rates using the Arrhenius equation with an activation energy E_a of 521 kJ kg^{-1} and a frequency factor A of 4.3×10^{24} were obtained by fitting to the data of Llana-Fúnez et al., (2007). The change in concentration of serpentine at each time step was used to determine the energy dissipated by dehydration using an enthalpy of reaction of 414 kJ kg^{-1} via Equation 3 where C is the concentration and n is the order of reaction. Experimental studies suggest that the order of reaction varies between 0.5 and 2.0 (Llana-Fúnez et al., 2007). A value of 1.0 was assumed in the current study. The transient heat flow was simulated using an implicit numerical integration with a time step of 1×10^{-9} s and an element size of 0.01 μm. Heat transfer by gas or melt migration is not considered in the model but is likely to be less important than conduction.

$$\frac{\partial C}{\partial t} = -C^n A \exp\left(-\frac{E_a}{RT}\right). \tag{3}$$

The results of the simulations suggest that serpentine dehydration produces a significant thermal gradient of up to 4000 K μm^{-1} after 0.01 s once surface melting occurs (Fig. 4). The temperature gradient shows a dependence on initial phyllosilicate abundance, however, even abundances of phyllosilicate of >5% maintain a large temperature gradient of 200 K μm^{-1}.

Thermal gradients of the magnitude predicted by the simulations would result in the fracturing of olivine crystals that penetrate the melt front into the unmelted core of a micrometeorite. The shear stress on crystals furthermore is largest at their surface suggesting that fractures will initiate at the exterior and then migrate inward. This agrees well with the observation that clusters of forsterite and enstatite within ScMMs often consist of several shard-like fragments surrounding a larger crystal.

IMPLICATIONS FOR INTERPLANETARY DUST AND THEIR PARENT BODIES

Thermal fracturing of forsterite and enstatite within ScMMs testifies to the presence of phyllosilicates within their precursor particles because they require large thermal gradients during entry heating (Genge, 2005). The abundance of fragmented olivine and enstatite within ScMMs suggests that 75% of their precursors contained at least 5 vol% phyllosilicates prior to atmospheric entry. The results imply, therefore, that the majority of ScMM precursors had experienced aqueous alteration and resemble CI1 and CM2 chondrites, rather than type 3 chondrites that have lower abundances of phyllosilicate (Brearley and Jones, 1998). This conclusion
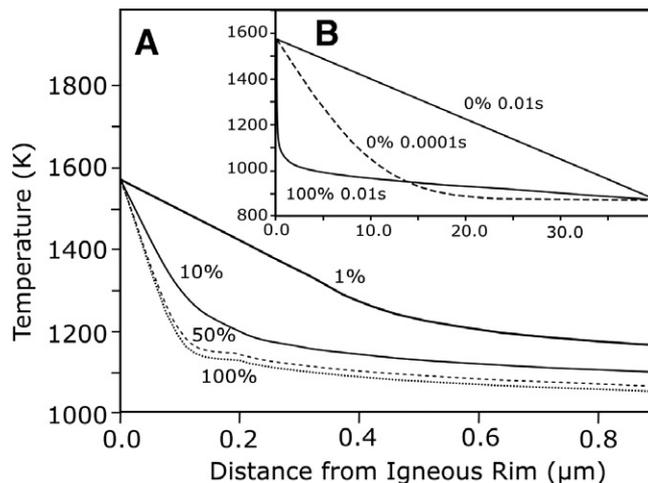
is compatible with previous suggestions that the precursors of ScMMs are equivalent to those of fine-grained MMs (Genge et al., 1997; Taylor et al., 2011). The majority of unmelted fine-grained MMs, however, are thermally altered and dominated by dehydroxylates after phyllosilicates, with still hydrated phyllosilicate being rare (Genge et al., 1997; Noguchi et al., 2002; Nozaki et al., 2006). It is, however, unclear whether the dehydration occurs during atmospheric entry or due to parent body processes.

Dehydration of phyllosilicates on asteroidal parent bodies can occur owing to parent body metamorphism (McSween et al., 2002), or shock (Rubin, 1995). The CK4 meteorite group is dominated by anhydrous silicates and has a matrix consisting largely of micron-scale olivines thought to have formed by dehydration and recrystallization of phyllosilicate by parent metamorphism (Greenwood et al., 2010). Up to 50% of CI and CM chondrites are also known to have experienced metamorphism with alteration of phyllosilicate to porously crystalline or amorphous phases (Tonui, 2014; Nakamura, 2005).

Shock experiments on CM2 chondrites at pressures >26 GPa indicate that phyllosilicate dehydration can be the result of collisions within the asteroid belt and results in explosive dispersal of hydrated primitive parent bodies (Tomeoka et al., 2003). The large abundance of CI1 and CM2 chondrite material amongst MMs, therefore, could be biased by the efficiency of dust production from such parent bodies. The occurrence of fragmented olivine suggests that maximum abundance of 25% of precursors contain <5 vol% phyllosilicate prior to atmospheric entry and thus extensive dehydration during dust production is relatively rare. By inference, explosive fragmentation is not the principle dust production mechanism from hydrated parent bodies.

The Veritas asteroid family is predicted to contribute ~50% of dust derived from asteroidal dust bands to Earth with the remainder largely derived from the Koronis family asteroids, perhaps together with a smaller contribution from the Themis family (Nesvorny et al., 2006). The relative abundance of MM types is broadly consistent with these asteroidal sources since although fine-grained unmelted particles, related to CI1 and CM2 chondrites, dominate at small size (<200 μm; Genge et al., 1997; Taylor et al., 2011), particles with affinities to ordinary chondrites comprise ~30% of larger (>300 μm) micrometeorites (Cordier et al., 2011; Van Ginneken et al., 2017) and are present among unmelted coarse-grained MMs (Genge, 2008). Koronis asteroids are S(IV) spectral types that are likely to be related to ordinary chondrites, while Veritas and Themis asteroids

are C or B types and likely to be related to the carbonaceous chondrites (Ziffer et al., 2011).

Fragmented olivine and enstatite in ScMMs indicate that their precursor dust grains contained abundant phyllosilicates as they entered Earth's atmosphere. Igneous rims on thermally altered fgMMs, likewise suggest that phyllosilicates were present (Genge, 2006). The likely parent bodies of these MMs, the Veritas and Themis family asteroids, thus contain abundant phyllosilicate in agreement with spectroscopic studies of these asteroids that show the presence of Ch type members of the families (Ziffer et al., 2011). The significant number of metamorphosed CI1 and CM2 chondrites, in contrast, may indicate different parent bodies for these meteorites.

CONCLUSIONS

Clusters of fractured Mg silicates within scoriaceous MMs are shown to form through fracturing due to thermal shock during entry heating. Thermal shock fracturing of forsterite is dependent on olivine crystal size but requires thermal gradients of several hundred degrees per micron that significantly exceed those generated by steady-state thermal conduction. Large thermal gradients sufficient to cause thermal fracturing of olivine can, however, be maintained by the endothermic decomposition of >5 vol% phyllosilicates. The presence of clusters of fractured olivine within ScMMS, therefore, indicate their precursors, prior to atmospheric entry contained phyllosilicate and, like fine-grained unmelted MMs, were probably similar to hydrated CM2 or CI chondrite matrix.

REFERENCES CITED
Bouhifd, M.A., Andrault, D., Fiquet, G., and Richet, P., 1996, Thermal expansion of forsterite up to the melting point: Geophysical Research Letters, v. 23, p. 1143–1146, doi:10.1029/96GL01118.

Brearley, A.J., and Jones, R.H., 1998, Chondritic meteorites, in Papike, J.J., ed., Planetary Materials: Mineralogical Society of America, v. 36, p. 1–191.

Brownlee, D.E., and Bates, B., 1983, Meteor ablation spherules as chondrule analogs in King, E. A., ed., Chondrules and Their Origins: Houston, Texas, Lunar and Planetary Institute, p. 10–25.

Cordier, C., Van Ginneken, M., and Folco, L., 2011, Nickel abundance in stony cosmic spherules: constraining precursor material and formation mechanisms: Meteoritics & Planetary Science, v. 46, p. 1110–1132, doi:10.1111/j.1945-5100.2011.01218.x.

Duprat, J., Engrand, C., Maurette, M., Kurat, G., Gounelle, M., and Hammer, C., 2007, Micrometeorites from central Antarctic snow: The CONCORDIA collection: Advances in Space Research, v. 39, p. 605–611, doi:10.1016/j.asr.2006.05.029.

Genge, M.J., 2008, Koronis asteroid dust in Antarctic ice: Geology, v. 36, p. 687–690, doi:10.1130/G24493A.1.

Genge, M.J., 2006, Igneous rims on micrometeorites: Geochimica et Cosmochimica Acta, v. 70, p. 2603–2621, doi:10.1016/j.gca.2006.02.005.

Genge, M.J., Grady, M.M., and Hutchison, R., 1997, The textures and compositions of fine-grained Antarctic micrometeorites—Implications for comparisons with meteorites: Geochimica et Cosmochimica Acta, v. 61, p. 5149–5162, doi:10.1016/S0016-7037(97)00308-6.

Genge, M.J., Engrand, C., Gounelle, M., and Taylor, S., 2008, The classification of micrometeorites: Meteoritics & Planetary Science, v. 43, p. 497–515, doi:10.1111/j.1945-5100.2008.tb00668.x.

Greenwood, R.C., Franchi, I.A., Kearsley, A.T., and Alard, O., 2010, The relationship between CK and CV chondrites: Geochimica et Cosmochimica Acta, v. 74, p. 1684–1705, doi:10.1016/j.gca.2009.11.029.

Kingery, W.D., 1955, Factors affecting thermal stress resistance of ceramic materials: Journal of the American Ceramic Society, v. 38, p. 3–15, doi:10.1111/j.1151-2916.1955.tb14545.x.

Kojima, T., Tomeoka, K., and Takeda, H., 1993, Unusual dark clasts in the Vigarano CV3 carbonaceous chondrite: Record of parent body process: Meteoritics & Planetary Science, v. 28, p. 649–658, doi:10.1111/j.1945-5100.1993.tb00636.x.

Kurat, G., Koeberl, C., Presper, T., Brandstatter, F., and Maurette, M., 1994, Petrology and geochemistry of Antarctic micrometeorites: Geochimica et Cosmochimica Acta, v. 58, p. 3879–3904, doi:10.1016/0016-7037(94)90369-7.

Llana-Fúnez, S., Brodie, K.H., Rutter, E.H., and Arkwrigt, J.C., 2007, Experimental dehydration kinetics of serpentinite using pore volumemetry: Journal of Metamorphic Geology, v. 25, p. 423–438, doi:10.1111/j.1525-1314.2007.00703.x.

Maurette, M., Olinger, C., Michel-Levy, M.C., Kurat, G., Pourchet, M., Brandstatter, F., and Bourot-Denise, M., 1991, A collection of diverse micrometeorites recovered from 100 tonnes of Antarctic blue ice: Nature, v. 351, p. 44–47, doi:10.1038/351044a0.

McSween, H.T., Ghosh, A., Grimm, R.E., Wilson, L., and Young, E.D., 2002. Thermal evolution models of Asteroids, in Bottke, W., ed., Asteroids III: Tucson, University of Arizona Press. p. 559.

Nakamura, T., 2005, Pos-hydration thermal metamorphism of carbonaceous chondrites: Journal of Mineralogical and Petrological Sciences, v. 100, p. 260–272, doi:10.2465/jmps.100.260.

Nesvorny, D., Vokrouhlicky, D., Bottke, W.F., and Sykes, M., 2006, Physical properties of asteroid dust bands and their sources: Icarus, v. 181, p. 107–144, doi:10.1016/j.icarus.2005.10.022.

Noguchi, R., et al., 2015, Cometary dust in Antarctic ice and snow: Past and present chondritic porous micrometeorites preserved on the Earth's surface: Earth and Planetary Science Letters, v. 410, p. 1–11, doi:10.1016/j.epsl.2014.11.012.

Noguchi, R., Nakamura, T., and Nozaki, W., 2002, Mineralogy of phyllosilicate-rich micrometeorites and comparison with Tagish Lake and Sayama meteorites: Earth and Planetary Science Letters, v. 202, p. 229–246, doi:10.1016/S0012-821X(02)00777-X.

Nozaki, W., Nakamura, T., and Noguchi, T., 2006, Bulk mineralogical changes of hydrous micrometeorites during heating in the upper atmosphere at temperatures below 1000°C: Meteoritics & Planetary Science, v. 41, p. 1095–1114, doi:10.1111/j.1945-5100.2006.tb00507.x.

Núñez-Valdez, M., Umemoto, K., and Wentzcovitch, R.M., 2010, Fundamentals of elasticity of (Mg1-x,Fex)2SiO4 olivine: Geophysical Research Letters, v. 37, L14308, doi:10.1029/2010GL044205.

Opeil, C.P., Consolmagno, S.J., Safarik, D.J., and Britt, D.T., 2012, Stony meteorite thermal properties and the relationship with meteorite chemical and physical states: Meteoritics & Planetary Science, v. 47, p. 319–329, doi:10.1111/j.1945-5100.2012.01331.x.

Rochette, P., Folco, L., Suavet, C., Van Ginneken, M., Gattacceca, J., Perchiazzi, N., Braucher, R., and Harvey, R.P., 2008, Micrometeorites from the Transantarctic Mountains: Proceedings of the National Academy of Sciences of the United States of America, v. 105, p. 18206–18211, doi:10.1073/pnas.0806049105.

Rubin, A.E., 1995, Petrologic evidence for collisional heating of chondritic asteroids: Icarus, v. 113, p. 156–167, doi:10.1006/icar.1995.1013.

Sammis, C.G., and Ben-Zion, Y., 2008, Mechanics of grain-size reduction in fault zones: Journal of Geophysical Research, v. 113, p. B02306, doi:10.1029/2006JB004892.

Suttle, M.D., Van Ginneken, M., and Genge, M.J., 2015. Larkman Nunatak micrometeorites, a statistical study 78th Annual Meeting of the Meteoritical Society, Berkeley, California, Abstract 1856.

Taylor, S., Lever, J.H., and Harvey, R.P., 2000, Numbers, types, and compositions of an unbiased collection of cosmic spherules: Meteoritics & Planetary Science, v. 35, p. 651–666, doi:10.1111/j.1945-5100.2000.tb01450.x.

Taylor, S., Matrajt, G., and Guan, Y., 2011, Fine-grained precursors dominate the micrometeorite flux: Meteoritics & Planetary Science, v. 47, p. 550–564, doi:10.1111/j.1945-5100.2011.01292.x.

Tomeoka, K., Kiriyama, K., Nakamura, K., Yamahana, Y., and Sekine, T., 2003, Interplanetary dust from the explosive dispersal of hydrated asteroids by impacts: Nature, v. 423, p. 60–62, doi:10.1038/nature01567.

Tonui, E., 2014, Petrographic, chemical and spectroscopic evidence for thermal metamorphism in carbonaceous chondrites I: CI and CM chondrites: Geochimica et Cosmochimica Acta, v. 126, p. 284–306, doi:10.1016/j.gca.2013.10.053.

Van Ginneken, M., Gattacceca, J., Rochette, P., Sonzogni, C., Alexandre, A., and Genge, M.J., 2017, The parent body controls on cosmic spherule texture: Evidence from the oxygen isotope composition of large micrometeorites: Geochimica et Cosmochimica Acta, doi:10.1016/j.gca.2017.05.008, (in press).

Yatsu, E., 1988. The Nature of Weathering: An introduction: Tokyo, Sozosha.

Ziffer, J., Campins, H., Licandro, J., Walker, M.E., Fernandez, Y., Clark, B.E., Mothe-Diniz, T., Howell, E., and Deshpande, R., 2011, Near-infrared spectroscopy of primitive asteroid families: Icarus, v. 213, p. 538–546, doi:10.1016/j.icarus.2011.04.008.